Global Change Biology

Global Change Biology (2011) **17**, 855–871, doi: 10.1111/j.1365-2486.2010.02274.x

Patterns of NPP, GPP, respiration, and NEP during boreal forest succession

M. L. GOULDEN*, A. M. S. McMILLAN[1]*, G. C. WINSTON*, A. V. ROCHA[2]*, K. L. MANIES†, J. W. HARDEN† and B. P. BOND-LAMBERTY‡

*Department of Earth System Science, University of California, Irvine, CA 92697-3100, USA, †US Geological Survey, 345 Middlefield Road, MS 962, Menlo Park, CA 94025, USA, ‡Pacific Northwest National Laboratory, Joint Global Change Research Institute at the University of Maryland – College Park, 5825 University Research Court, Suite 3500, College Park, MD 20740, USA

Abstract

We combined year-round eddy covariance with biometry and biomass harvests along a chronosequence of boreal forest stands that were 1, 6, 15, 23, 40, ~74, and ~154 years old to understand how ecosystem production and carbon stocks change during recovery from stand-replacing crown fire. Live biomass (C_{live}) was low in the 1- and 6-year-old stands, and increased following a logistic pattern to high levels in the 74- and 154-year-old stands. Carbon stocks in the forest floor ($C_{forest\ floor}$) and coarse woody debris (C_{CWD}) were comparatively high in the 1-year-old stand, reduced in the 6- through 40-year-old stands, and highest in the 74- and 154-year-old stands. Total net primary production (TNPP) was reduced in the 1- and 6-year-old stands, highest in the 23- through 74-year-old stands and somewhat reduced in the 154-year-old stand. The NPP decline at the 154-year-old stand was related to increased autotrophic respiration rather than decreased gross primary production (GPP). Net ecosystem production (NEP), calculated by integrated eddy covariance, indicated the 1- and 6-year-old stands were losing carbon, the 15-year-old stand was gaining a small amount of carbon, the 23- and 74-year-old stands were gaining considerable carbon, and the 40- and 154-year-old stands were gaining modest amounts of carbon. The recovery from fire was rapid; a linear fit through the NEP observations at the 6- and 15-year-old stands indicated the transition from carbon source to sink occurred within 11–12 years. The NEP decline at the 154-year-old stand appears related to increased losses from C_{live} by tree mortality and possibly from $C_{forest\ floor}$ by decomposition. Our findings support the idea that NPP, carbon production efficiency (NPP/GPP), NEP, and carbon storage efficiency (NEP/TNPP) all decrease in old boreal stands.

Keywords: black spruce, chronosequence, fire, gross primary production, net ecosystem production, net primary production, *Picea mariana*, secondary succession

Received 2 April 2010 and accepted 6 May 2010

Introduction

The patterns and controls on plant succession have interested ecologists for more than a century (Clements, 1916), and extensive bodies of work have accumulated on both the biological controls on recovery (e.g. Connell & Slatyer, 1977) and the implications of recovery for ecosystem function (e.g. Odum, 1969; Bormann & Likens, 1979). More recently, research has focused on the effects of disturbance and recovery on carbon (e.g. Houghton *et al*., 1983) and energy (e.g. Randerson *et al*., 2006) exchange, with the goals of understanding the contemporary terrestrial carbon cycle and predicting the climate forcing caused by possible future changes in disturbance regime (e.g. Hurtt *et al*., 2002).

Several conceptual models have been proposed to describe the recovery of forest production and biomass from disturbance (Kira & Shidei, 1967; Odum, 1969; Bormann & Likens, 1979; Sprugel, 1985; Waring & Schlesinger, 1985; Ryan *et al*., 1997; Chapin *et al*., 2002). Sprugel (1985) provides an overview of the expected changes in carbon stocks during regrowth (Fig. 1a), which draws on the findings at and around Hubbard Brook (Vitousek & Reiners, 1975; Bormann & Likens, 1979; Covington, 1981). Disturbance reduces live biomass and increases the amount of carbon in the coarse woody debris (C_{CWD}) and the forest floor ($C_{forest\ floor}$). This detritus subsequently decomposes, resulting in declining detrital stocks, while plant production recovers, resulting in gradually increasing live biomass (C_{live}). The loss of detritus, especially from the forest

[1]Present address: A. M. S. Mcmillan, National Institute of Water and Atmospheric Research, Wellington, New Zealand.

[2]Present address: A. V. Rocha, Marine Biological Laboratory Ecosystems Center, Woods Hole, MA 02543, USA.

Correspondence: M. L. Goulden, e-mail: mgoulden@uci.edu

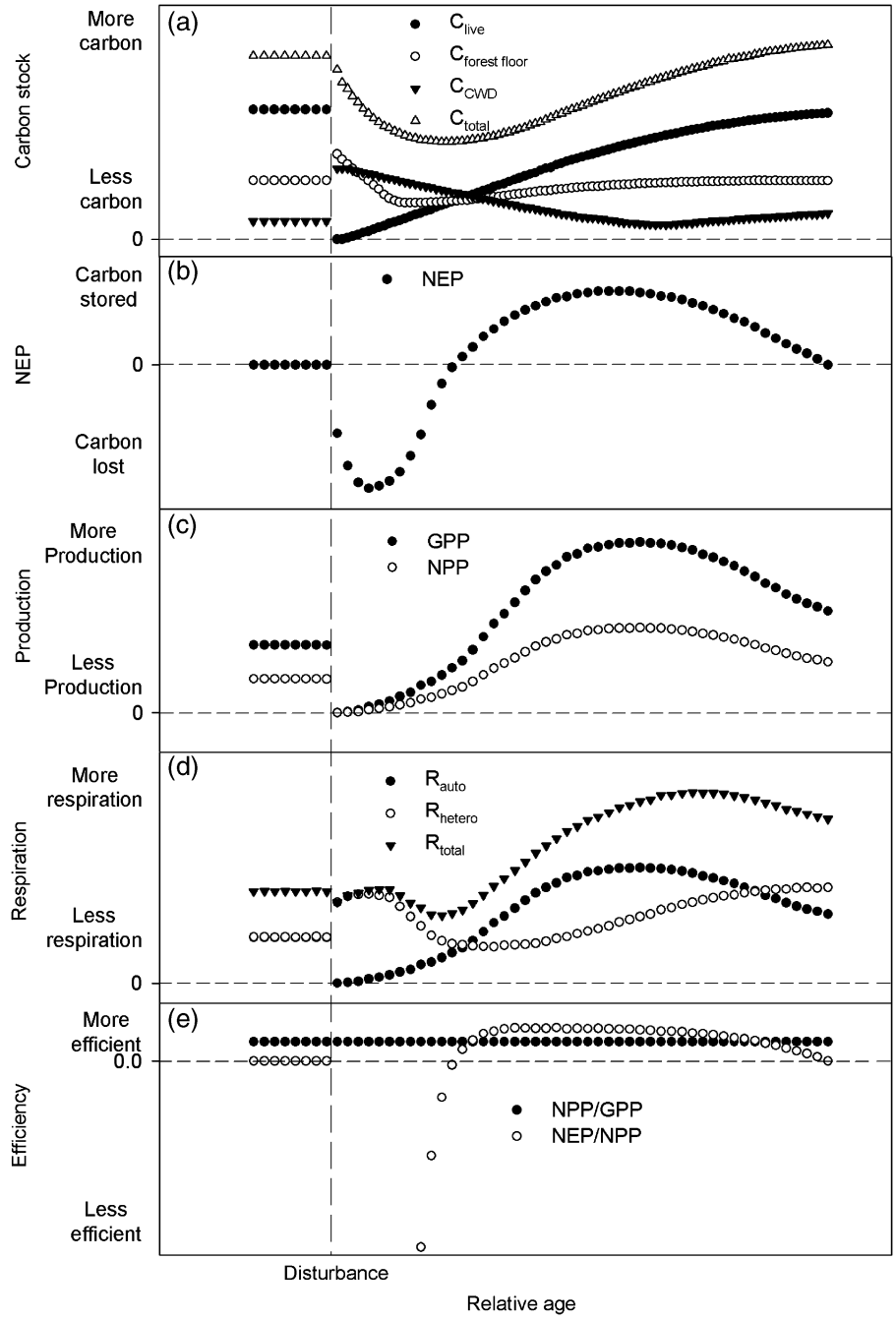

Fig. 1 Hypothesized trends in biomass and production during secondary succession. (a) Live biomass (C_{live}), forest floor ($C_{forest\ floor}$), coarse woody debris (C_{CWD}), and total live biomass (C_{total}; all digitized from Sprugel, 1985's Fig. 2). (b) Net ecosystem production (NEP; digitized from Chapin *et al*., 2002's Fig. 13.11). (c) Gross primary production (GPP) and net primary production (NPP; all digitized from Chapin *et al*., 2002's Fig. 13.9). (d) Autotrophic respiration (R_{auto}), heterotrophic respiration (R_{hetero}), and total respiration (R_{total}; all digitized or calculated from Chapin *et al*., 2002's Figs 13.9 and 13.11). (e) Plant production efficiency (NPP/GPP) and ecosystem carbon storage efficiency (NEP/NPP; calculated from Chapin *et al*., 2002's Figs 13.9 and 13.11). The time of disturbance is indicated by the dashed vertical line.

floor, is thought to proceed more rapidly than the accumulation of live biomass, resulting in an initial loss of total carbon (C_{total}) and driving a net efflux of CO_2 to the atmosphere (a negative Net ecosystem production or NEP; see Fig. 1a and b). Over time, plant growth and biomass accumulation increase, and the input of new

litter causes the detrital pools to build up, resulting in an extended period of carbon accumulation and a positive NEP. Finally, the buildup of C_{live}, $C_{forest\ floor}$, and C_{CWD} cause mortality and decomposition losses to accelerate, which moves the pools toward steady state and causes NEP to approach zero in the oldest stands (Odum, 1969).

Chapin *et al*. (2002) expanded this model to consider the successional changes in gross primary production (GPP; the annual carbon fixation by autotrophs), net primary production (NPP; the annual growth by autotrophs), autotrophic respiration (R_{auto}; the annual respiration by autotrophs), and heterotrophic respiration (R_{hetero}; the annual respiration by heterotrophs). Chapin and colleagues hypothesized NPP varies markedly during recovery, reaching a peak in middle age, and declining by as much as 50% in old stands (Fig. 1c). Chapin and colleagues further hypothesized the changes in NPP with age are driven exclusively by changes in GPP (Fig. 1c), and that the NPP to GPP ratio remains constant, with R_{auto} tracking NPP and GPP (Fig. 1d and e). The observation that forest NPP peaks in mid-succession is well established (Kira & Shidei, 1967; Ryan *et al*., 1997; Bond-Lamberty *et al*., 2004; Mack *et al*., 2008), whereas the hypothesis that the NPP to GPP ratio remains constant is more recent (Ryan *et al*., 1997; Waring *et al*., 1998) and marks a departure from early work that attributed NPP trends almost exclusively to increasing R_{auto} (Waring & Schlesinger, 1985) or a combination of decreasing GPP and increasing R_{auto} (Kira & Shidei, 1967).

The changes in biomass and production with stand age are most effectively investigated using a chronosequence, or space for time, approach (Harden *et al*., 1997; Law *et al*., 2003; Litvak *et al*., 2003; Bond-Lamberty *et al*., 2004; Clark *et al*., 2004; Amiro *et al*., 2006; Goulden *et al*., 2006; Humphreys *et al*., 2006; Randerson *et al*., 2006; Noormets *et al*., 2007; Mkhabela *et al*., 2009; Zha *et al*., 2009). The boreal forest provides an ideal system to investigate the changes in production and carbon stocks with recovery. Lightning caused crown fires occur at individual locations about once every 100 years, resulting in a mosaic of large patches at different stages of succession (Van Cleve *et al*., 1983; Bonan & Shugart, 1989). We combined year-round eddy covariance measurements with *in situ* observations of carbon stocks and production along a fire-recovery chronosequence in Manitoba, Canada to investigate the patterns of NPP, GPP, respiration, and NEP during boreal forest succession. Our goals were to better develop the methods and strategy to investigate the changes in carbon pools and fluxes during succession and to explicitly test the trends predicted by Sprugel (1985) and Chapin *et al*. (2002).

Methods

Sites

We focused on a chronosequence in central Manitoba that included seven even-aged boreal forest stands at various stages of succession (Table 1; Bond-Lamberty *et al*., 2004; Goulden *et al*., 2006). The ages of the oldest two burns (1850 and 1930) were determined by coring black spruce; the ages of the younger stands were determined from fire records. For simplicity, we refer to the age of each site in 2004, even though some of the observations were made in other years and the Figures reflect the actual age at observation. Most of the observations were made at the University of California, Irvine (UCI) sites, using methods described here or in Goulden *et al*. (2006). A few of the observations were made at the University of Wisconsin (UW) sites, using methods described in Bond-Lamberty *et al*. (2004) and Wang *et al*. (2003). The UCI and UW sites were located in the same burn scars and were no more than 3 km apart. The methods used at NOBS-1850 are described in Goulden *et al*. (1997) and Dunn *et al*. (2007). The study was conducted in the area of the BOReal Ecosystem–Atmosphere Study (BOREAS) Northern Study Area (NSA; Sellers *et al*., 1997); many additional data sets from the BOREAS project are available (http://daac.ornl.gov/).

Carbon stocks, NPP and leaf area index (LAI)

The aboveground biomass and LAI (Table 2) of herbaceous plants (principally grasses and forbs and not including mosses) was determined at each UCI site (Table 1) in September 2004 by harvest. The harvests occurred shortly before the end of the growing season and were assumed to reflect peak biomass, peak LAI, and annual aboveground NPP (ANPP). The herbaceous material in 30 to 40 0.25 m^2 plots at 10 m intervals along 100 m transects radiating in the cardinal directions from the eddy covariance towers was clipped, returned to the lab, dried at 65 °C, and weighed. Subsamples were sorted into deciduous leaves, new evergreen leaves, and old evergreen leaves. LAI was calculated as the product of this leaf biomass and the specific leaf area (SLA) for individual species, which was measured at the UW sites (Bond-Lamberty *et al*., 2002b).

Wood production of saplings and shrubs was calculated for individual plants based on basal diameter, ring width, and species-specific allometric equations. The basal stem diameter (at the soil surface) of the understory shrubs and tree saplings at the UCI sites was measured with vernier calipers in 13–40 1 m^2 plots along the transects. The biomass, new leaf production, and LAI of understory tree saplings [jack pine (*Pinus banksiana* [Lamb.]), aspen (*Populus tremuloides* [Michx.]), black spruce (*Picea mariana* [Mill.]), and willow (*Salix* spp.)] were calculated with species-specific allometric equations from Bond-Lamberty *et al*. (2002a) and SLAs from Bond-Lamberty *et al*. (2002b). The biomass and LAI of alder (*Alnus* spp.), which Bond-Lamberty and colleagues did not investigate, were calculated with allometric equations that we developed between basal diameter, biomass, and the mass of leaves by harvesting

Table 1 Study sites

	Location	*Conditions in summer 2005*
UCI-2003	55°53′53″ 98°12′58″	Rapidly developing herbaceous layer of wild rose (*Rosa* spp.), fireweed (*Epilobium angustifolium* L.), grass, Labrador tea (*Ledum groenlandicum* Oeder), alder (*Alnus crispa*), willow (*Salix spp.*), poplar, and aspen (*Populus tremuloides* Michx). Many 2–4 cm tall black spruce (*Picea mariana*) and jack pine (*Pinus banksiana* Lamb.) seedlings. Almost all of the black spruce trees killed in the 2003 fire were still standing
UCI-1998	56°38′9″ 99°56′54″	Thick, patchy layer of fireweed, wild rose, grass, Labrador tea, alder, and patchy firemoss. Many 10–25 cm tall black spruce. Almost all of the black spruce trees killed in the 1998 fire were still standing
UW-D1998	56°37′41″ 99°56′31″	3 km south of UCI-1998. Wetter with more sphagnum moss than UCI-1998
UCI-1989	55°55′0″ 98°57′52″	Thick layer of wild rose, grass, Labrador tea, fireweed, alder, and willow. Extensive firemoss with patches of sphagnum (*Sphagnum* spp.) and feather (*Ptilium*, *Pleurozium*, or *Hylocomium* spp.) moss. Many 20–100 cm tall black spruce, 100–200 cm tall jack pine, and 50–400 cm aspen. Most black spruce trees killed by the 1989 fire fell from 2000 to 2005
UW-D1989	55°54′23″ 98°58′46″	1.5 km southwest of UCI-1989. Similar vegetation, steeper and more southerly aspect than UCI-1989
UCI-1981	55°51′47″ 98°29′6″	Dense stand of 500 cm tall jack pine with scattered 500 cm tall aspen. Many 100–200 cm tall black spruce. Continuous ground cover of grass, Labrador tea, willow, and wild rose. Mix of sphagnum and feather moss, Most black spruce trees killed by the 1981 fire had fallen before 2000
UW-D1981	55°51′50″ 98°28′57″	75 m east of UCI-1981. Similar to UCI-1981
UCI-1964	55°54′42″ 98°22′56″	Moderately dense stand of 500–700 cm tall jack pine and aspen, with significant mortality and thinning. Many 200–600 cm tall black spruce. Ground cover of feather moss with sparse grass
UW-D1964	55°55′12″ 98°39′21″	1.5 km northwest of UCI-1964. More deciduous, larger trees than UCI-1964
UCI-1930	55°54′21″ 98°31′29″	Closed canopy of 12–20 m tall black spruce, with a few senescent jack pine and aspen. Nearly 100% feather moss cover. Significant shrub layer of alder, willow, and Labrador tea
UW-D1930	55°54′29″ 98°31′9″	500 m northeast of UCI-1930. Similar to UCI-1930
UCI-1850	55°52′45″ 98°29′2″	Closed canopy of 14–18 m tall black spruce. Nearly 100% feather moss cover. Open understory with a few alders, Labrador tea, and willow. Tower is centered in a well-drained, slightly upland area
UW-D1850	55°52′45″ 98°28′48″	400 m east of UCI-1850. Similar to UCI-1850
NOBS-1850	55°52′45″ 98°28′48″	NOBS tower is 400 m east of UCI-1850 tower. NOBS tower samples both well- and poorly drained areas

UCI, University of California, Irvine; UW, University of Wisconsin.

103 alder shrubs across the UCI sites. The annual basal diameter increment of the understory shrubs and tree saplings was determined on cross sectional discs cut from stems in the 1 m^2 plots (266 discs at UCI-1998, 212 discs at UCI-1989, 132 discs at UCI-1981, 94 discs at UCI-1964, 44 discs at UCI-1930, and 33 discs at UCI-1850).

Overstory tree diameters at breast height (DBH; 1.3 m) were measured in three or four 25–50 m^2 plots in the cardinal directions from the eddy covariance tower at each of the UCI sites (100 m^2 total at UCI-1989, 75 m^2 total at UCI-1981, 100 m^2 total at UCI-1964, 150 m^2 total at UCI-1930, and 150 m^2 total at UCI-1850). The overstory biomass and LAI of each species at each site was calculated with species-specific allometric equations from Bond-Lamberty *et al*. (2002a) and SLAs from Bond-Lamberty *et al*. (2002b). Wood production was determined from ring width. Trees of the dominant species at each site were cored twice (on the north and west aspect of the tree) at breast height (DBH; 1.3 m) with an increment borer (Rocha *et al*., 2006; 35 trees cored at UCI-1989, 101 trees at UCI-1981, 88 trees at UCI-1964, 117 trees at UCI-1930, and 96 trees at UCI-1850). The cores were sanded and scanned at 1200 dpi, and the ring widths determined with LIGNOVISION software (Rinntech, Heidelberg, Germany). Wood and leaf production were calculated based on measured DBH, ring width in 2004, and species-specific allometric equations (Bond-Lamberty *et al*., 2002a). The rates of individual tree production were summed for the plot to calculate the annual leaf and wood production.

Belowground fine, medium, and coarse root production (BNPP; Table 2) was determined by sequential coring at each of the UW sites (Bond-Lamberty *et al*., 2004). Twenty 16.6 $cm^2 \times 50$ cm deep cores were taken and sorted at each site in July and October 2001. Moss NPP at the UCI sites was

Table 2 Ecosystem fluxes, stocks and properties

	What	How
LAI	Leaf area index	Measured at the UCI sites by harvest and allometry
ANPP	Aboveground net primary production	Calculated as the sum of vascular and moss NPP at the UCI sites
BNPP	Belowground net primary production	Measured at the UW sites by sequential coring
TNPP	Total net primary production	Calculated as the sum of aboveground vascular and moss NPP at the UCI sites and root production at the UW sites
C_{live}	Carbon stocks in live plants	Calculated as the sum of vascular and moss biomass at the UCI sites
$C_{forest\ floor}$	Carbon stocks in the forest floor	Measured at the UCI sites by harvest
C_{CWD}	Carbon stocks in coarse woody debris	Measured at the UCI sites by line intercept
C_{total}	Total carbon stocks excluding the soil	Calculated as the sum of C_{live}, $C_{forest\ floor}$, and C_{CWD} at the UCI sites
R_{total}	Total ecosystem respiration	Calculated by integrated eddy covariance at the UCI sites using a u^* filter of $0.3\,ms^{-1}$ and daytime extrapolation based on air temperature
GPP	Gross primary production	Calculated by integrated daytime eddy covariance at the UCI sites after subtracting R_{total}
NEP_{EC}	Net ecosystem production determined by Eddy covariance	Calculated at the UCI sites using a u^* filter of $0.3\,ms^{-1}$
NEP_{stocks}	Net ecosystem production determined by change in C_{total} between sites	Calculated as the difference in C_{total} between sequentially aged stands divided by the age difference
NEP_{NPP}	Net ecosystem production determined by the difference between NPP and decomposition	Calculated as the difference between TNPP and decomposition at the UW sites (Bond-Lamberty *et al*., 2004). Decomposition at the UW sites was determined with measurements of soil respiration in trenched plots
R_{auto}	Annual plant respiration	Calculated as the difference between GPP and TNPP
R_{hetero}	Annual heterotrophic respiration	Calculated as the difference between TNPP and NEP_{EC}
TNPP/GPP	Total primary production efficiency	Calculated as TNPP divided by GPP
ANPP/GPP	Aboveground primary production efficiency	Calculated as ANPP divided by GPP
NEP/TNPP	Carbon storage efficiency	Calculated as NEP_{EC} divided by TNPP

UCI, University of California, Irvine; UW, University of Wisconsin.

measured in 2004 using a combination of florescent dye (Harden *et al*., 2009), natural markers (Callaghan *et al*., 1978), and the crank wire technique (Clymo, 1970). Site specific new growth by species, as measured by one of the three methods, was multiplied by species cover at each site (Harden *et al*., 2009). Moss growth was not measured at the 23-year-old stand, and the average species growth rate across all of the other sites was used.

Coarse woody debris stock (C_{CWD}; Table 2) was measured at each of the UCI sites by the line intercept method using 18–20 20 m long transects (Manies *et al*., 2005). Forest floor carbon stock ($C_{forest\ floor}$; Table 2; dead moss, leaf litter, fine debris, and partially decomposed organic material above the mineral soil) and live moss biomass were measured at each of the UCI sites. We measured the thickness of organic soil layers every 3–20 m along two or more linear transects at each site. We collected samples from the L (live moss), D (dead moss), F (fibric), M (mesic), and H (humic) horizons at a series of soil pits along the transects (Manies *et al*., 2006). Cumulative carbon storage for all layers above the mineral soil was calculated as bulk density multiplied by %C and by the thickness of the horizon.

Total NPP (TNPP; Table 2) was calculated as the sum of aboveground vascular and moss NPP at the UCI sites and root production at the UW sites (Table 2). ANPP (Table 2) was calculated as the sum of vascular and moss NPP at the UCI sites. Live biomass (C_{live}; Table 2) was calculated as the sum of vascular and moss biomass at the UCI sites. Total carbon (C_{total}; Table 2) was calculated as the sum of C_{live}, $C_{forest\ floor}$, and C_{CWD} at the UCI sites.

NEP by change in stocks (NEP_{stocks}; Table 2) was calculated as the sequential difference in C_{total} between the 154-, 74-, 40-, 23-, and 6-year-old UCI stands divided by the age difference between stands. NEP by the difference between NPP and decomposition (NEP_{NPP}; Table 2) was calculated as the difference between NPP at the UW sites and decomposition at the UW sites (Bond-Lamberty *et al*., 2004). Decomposition at the UW sites was determined by combining chamber-based measurements of soil respiration for plots that had been trenched to exclude live roots with field- and laboratory-based measurements of woody debris heterotrophic respiration (Bond-Lamberty *et al*., 2004).

Meteorological and tower fluxes

Eddy covariance towers were installed at the UCI sites in summer 2001, 2002, or 2003 and operated until September 2005. Matched instruments and programs were used, which maximized site-to-site precision and allowed us to operate the tower network in an efficient manner (Goulden *et al*., 2006).

The CO_2 fluxes were calculated as the 30 min covariance of vertical wind velocity and CO_2 mixing ratio. Wind and temperature were measured with three-axis sonic anemometers (CSAT3, Campbell Scientific, Logan UT, USA); the molar concentrations of CO_2 and H_2O were measured with closed path IRGAs (LI7000, LiCor, Lincoln, NE, USA). The IRGAs were calibrated automatically for CO_2 once a week by sequentially sampling CO_2 and H_2O scrubbed air and CO_2 standard in air ($\pm$ 1%, Scott Marin, Riverside, CA, USA). Net radiation (REBS Q*7.1, Seattle, WA, USA), incoming and reflected shortwave radiation (CM3, Kipp and Zonen, Delft, the Netherlands), incoming and reflected photosynthetically active photon flux density (PPFD) (SZ-190, LiCor), and aspirated air temperature and relative humidity (HMP45C, Vaisala, Helsinki, Finland) were measured at the tower tops. The tower infrastructure at UCI-2003 differed somewhat from the other sites; UCI-2003 was installed after the main study had started, and budget constraints restricted measurements there to the growing season.

The annual tower fluxes at the UCI sites were calculated from October 1 to September 30 of each year by summing continuous, gap-filled time series that accounted for data loss from instrument failure and inadequate turbulence. Nocturnal respiration and NEP by integrated eddy covariance (NEP_{EC}; Table 2) were calculated using a u^* filter of 0.3 ms^{-1}. Total respiration (R_{total}) was calculated by extrapolating the nocturnal observations of respiration to daytime based on air temperature. GPP was calculated by integrating the daytime eddy covariance observations after subtracting the extrapolated rates of respiration. The measurements at UCI-2003 site were restricted to the summer, and the annual fluxes there were estimated based on the winter observations at the other young sites. The annual tower fluxes at NOBS-1850 were calculated from January 1 to December 31 of each year as described by Dunn *et al.* (2007).

The use of u^* filters (Goulden *et al.*, 1996) remains somewhat controversial, though there is consensus some type of correction on calm nights is needed (Finnigan, 2008). We investigated the sensitivity of NEP_{EC} to u^* threshold for the six sites with year-round fluxes by sequentially calculating NEP_{EC} at u^*s of 0, 0.1, 0.15, 0.2, 0.225, 0.25, 0.3, and 0.4 ms^{-1} (Fig. 2). NEP_{EC} initially decreased with an increasing u^* filter at all sites. NEP_{EC} reached a plateau at a filter of $\sim$0.2 ms^{-1} at some sites (1998, 1981) and a filter of $\sim$0.3 ms^{-1} at other sites (1930, 1850). The degree of site-to-site variation, as well as the general relationship, is typical of reports in the literature. There was no systematic trend in behavior; sites that required a higher filter included UCI-1989, which had a relatively open and short canopy, and UCI-1850, which had one of the densest and tallest canopies. The slope of u^* vs. NEP_{EC} was consistent between sites, making the site-to-site patterns of NEP_{EC} largely independent of the threshold selected. We used a u^* filter of 0.3 ms^{-1} for all data processing; all of the sites reached a plateau by this point, decreasing by no more than 14 g C m^{-2} yr^{-1} in response to an incremental increase from 0.3 to 0.4 ms^{-1} (Fig. 2).

We created a modeled respiration data set based on the relationship between air temperature and nighttime efflux. We recalculated the temperature sensitivity term in the model at

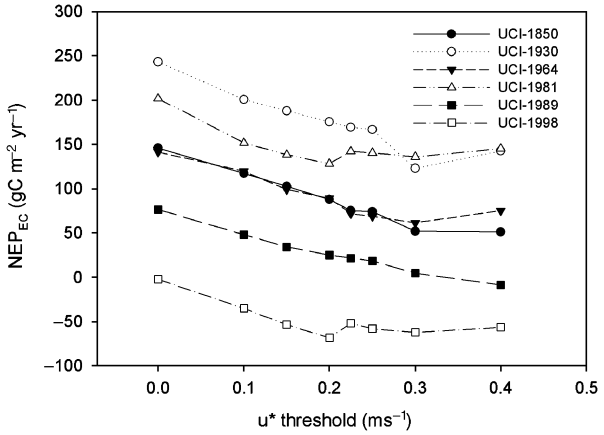

Fig. 2 Effect of u^* filter criteria on calculated NEP_{EC} (g C m^{-2} yr^{-1}) for October 2002 to September 2004 at the six chronosequence stands with year-round observations. NEP_{EC} is presented in the ecological sign convention, with a positive flux indicating the net transfer of carbon from the atmosphere to the ecosystem. NEP, net ecosystem production.

5-day intervals (Reichstein *et al.*, 2005). Gaps at night were filled with the modeled respiration data set. Gaps during the day were filled using modeled daytime net uptake calculated from a three parameter hyperbolic fit between CO_2 uptake and incoming PPFD (Falge *et al.*, 2001). Two-month time windows were used for the CO_2 uptake regressions. Gaps during periods when regression statistics indicated a poor fit ($r^2 < 0.1$ at night or $r^2 < 0.4$ during daytime) were filled by diel look-up tables and/or linear interpolation. The gap filling for daytime uptake was done over a series of temperature ranges to account for the effect of temperature on photosynthetic light response.

The flux tower analysis emphasizes data from October 2002 to September 2004, since these years had the most continuous observations (Goulden *et al.*, 2006) and since the site-to-site patterns of exchange during these years were similar to those observed in the other years (McMillan *et al.*, 2008). The final data sets are available from the authors (http://www.ess.uci.edu/ $\sim$ boreal_canada/index.html) and the AmeriFlux Data Archive (http://public.ornl.gov/ameriflux/data-access-select.shtml). The raw data are available from the authors.

Uncertainty

We provide our best estimates of uncertainty in Table 3, which draws heavily on our previous work. Sources of uncertainty are divided into: (1) Measurement and aggregation error, such as that caused by poorly calibrated instruments or by within-site spatial variability or by day-to-night biases in the calculation of eddy covariance sums (Goulden *et al.*, 1996; Bond-Lamberty *et al.*, 2004). (2) Site-to-site and year-to-year imprecision, such as that caused by the inconsistent application of a technique from one site to another or by measurement drift over time (Goulden *et al.*, 1996, 2006). (3) Across landscape sampling error, such as that caused by stand-to-stand or

Table 3 90% confidence intervals for ecosystem fluxes, stocks and properties

	Measurement and aggregation accuracy	Site-to-site and year-to-year precision	Across landscape sampling accuracy	Temporal sampling accuracy
LAI	$1\,m^2\,m^{-2}$*	$1\,m^2\,m^{-2}$*	$2\,m^2\,m^{-2}$†,‡	$1\,m^2\,m^{-2}$§
C_{live}	$500\,g\,C\,m^{-2}$*	$500\,g\,C\,m^{-2}$*	$1000\,g\,C\,m^{-2}$†,‡	$100\,g\,C\,m^{-2}$¶
$C_{forest\ floor}$	$500\,g\,C\,m^{-2}$*	$500\,g\,C\,m^{-2}$*	$1000\,g\,C\,m^{-2}$‡	Unknown
C_{CWD}	$300\,g\,C\,m^{-2}$*	$300\,g\,C\,m^{-2}$*	$2000\,g\,C\,m^{-2}$‡	$100\,g\,C\,m^{-2}$¶
C_{total}	$800\,g\,C\,m^{-2}$*,‖	$800\,g\,C\,m^{-2}$*,‖	$2500\,g\,C\,m^{-2}$†,‡,‖	$150\,g\,C\,m^{-2}$¶,‖
ANPP	$30\,g\,C\,m^{-2}\,yr^{-1}$*	$30\,g\,C\,m^{-2}\,yr^{-1}$*	$100\,g\,C\,m^{-2}\,yr^{-1}$†,‡	$50\,g\,C\,m^{-2}\,yr^{-1}$§,¶
BNPP	$75\,g\,C\,m^{-2}\,yr^{-1}$*	$75\,g\,C\,m^{-2}\,yr^{-1}$*	Unknown	Unknown
TNPP	$80\,g\,C\,m^{-2}\,yr^{-1}$*,‖	$80\,g\,C\,m^{-2}\,yr^{-1}$*,‖	$150\,g\,C\,m^{-2}\,yr^{-1}$†,‡,‖	$75\,g\,C\,m^{-2}\,yr^{-1}$§,¶,‖
R_{total}	$200\,g\,C\,m^{-2}\,yr^{-1}$*,**,††	$50\,g\,C\,m^{-2}\,yr^{-1}$*,**,††	Unknown	$100\,g\,C\,m^{-2}\,yr^{-1}$‡‡
GPP	$100\,g\,C\,m^{-2}\,yr^{-1}$*,**	$50\,g\,C\,m^{-2}\,yr^{-1}$*,**	$200\,g\,C\,m^{-2}\,yr^{-1}$†	$100\,g\,C\,m^{-2}\,yr^{-1}$§,‡‡
NEP_{EC}	$50\,g\,C\,m^{-2}\,yr^{-1}$*,**,††	$30\,g\,C\,m^{-2}\,yr^{-1}$*,**,††	Unknown	$50\,g\,C\,m^{-2}\,yr^{-1}$‡‡
NEP_{stocks}	$20\,g\,C\,m^{-2}\,yr^{-1}$*,‖	$20\,g\,C\,m^{-2}\,yr^{-1}$*,‖	$150\,g\,C\,m^{-2}\,yr^{-1}$†,‡	$5\,g\,C\,m^{-2}\,yr^{-1}$¶,‖
NEP_{NPP}	$50\,g\,C\,m^{-2}\,yr^{-1}$*,**,††	$20\,g\,C\,m^{-2}\,yr^{-1}$*,‖	$100\,g\,C\,m^{-2}\,yr^{-1}$†,‡	Unknown
R_{auto}	$125\,g\,C\,m^{-2}\,yr^{-1}$*,**,‖	$95\,g\,C\,m^{-2}\,yr^{-1}$*,**,‖	Unknown	$50\,g\,C\,m^{-2}\,yr^{-1}$‡‡,‖
R_{hetero}	$95\,g\,C\,m^{-2}\,yr^{-1}$*,**,‖	$85\,g\,C\,m^{-2}\,yr^{-1}$*,**,‖	Unknown	$50\,g\,C\,m^{-2}\,yr^{-1}$‡‡,‖
TNPP/GPP	0.2‖	0.2‖	Unknown	Unknown
ANPP/GPP	0.1‖	0.1‖	Unknown	Unknown
NEP/TNPP	0.2‖	0.2‖	Unknown	Unknown

*Based on instrument specifications, measurement repeatability, and within-site sampling variability.
†Based on spatial satellite observations (McMillan & Goulden, 2008; Goulden *et al*., 2006).
‡Based on between site sampling variability (Bond-Lamberty *et al*., 2004; Bond-Lamberty & Gower, 2008).
§Based on interannual satellite observations (McMillan & Goulden, 2008; Goulden *et al*., 2006).
¶Based on tree ring chronologies or multiyear sampling (Bond-Lamberty *et al*., 2004; Rocha *et al*., 2006).
‖Based on propagation of component uncertainties.
**Based on sensitivity analysis during aggregation process (e.g., Goulden *et al*., 1996).
††Based on comparisons with independent measures.
‡‡Based on measured interannual and decadal variability at all UCI sites and NOBS-1850 (McMillan *et al*., 2008; Dunn *et al*., 2007).
LAI, leaf area index; C_{live}, carbon stocks in live plants; $C_{forest\ floor}$, carbon stocks in the forest floor; C_{CWD}, carbon stocks in coarse woody debris; ANPP, aboveground net primary production; BNPP, belowground net primary production; TNPP, total net primary production; GPP, gross primary production; NEP_{EC}, net ecosystem production determined by Eddy covariance; NEP_{stocks}, net ecosystem production determined by change in C_{total} between sites; NEP_{NPP}, net ecosystem production determined by the difference between NPP and decomposition; R_{auto}, annual plant respiration; R_{hetero}, annual heterotrophic respiration.

burn-to-burn heterogeneity (Bond-Lamberty *et al*., 2004; Goulden *et al*., 2006). (4) Temporal sampling error, such as that caused by interannual or decadal variability that results in an anomalous measurement period (Dunn *et al*., 2007).

Ninety percent confidence intervals are expressed in absolute physical units. In some cases, the uncertainties are highly subjective (e.g., the accuracy of R_{auto} and R_{hetero}). In other cases, especially involving spatial sampling, there is insufficient information to even allow an estimate. Relatively simple measures of vegetation density, such as LAI, ANPP, and C_{live}, have low measurement and aggregation errors and good precision. The greatest uncertainty for these measures is caused by spatial heterogeneity across the landscape. More complex measures, especially those involving nocturnal eddy covariance fluxes (e.g., R_{total}), have large measurement and aggregation uncertainty and somewhat more favorable precision.

Site-to-site precision is most important for comparing between sites (e.g., determining whether one site is different from another). Site-to-site precision and spatial sampling error are most important for assessing how ecosystem properties change during succession (e.g., determining how NEP changes during succession). Measurement and aggregation errors, spatial sampling errors, and temporal sampling errors are most important when comparing the observations with independent information (e.g., using the observations to test a model or develop a regional carbon budget). Readers are urged to keep these issues in mind as they evaluate and use the data.

Sign convention

Annual production (i.e. NPP, NEP, GPP) is presented in the ecological sign convention, where a positive flux indicates the net transfer of carbon from the atmosphere to the ecosystem. Half-hour eddy covariance fluxes are presented in the atmospheric sign convention, where a positive flux indicates the net transfer of carbon from the ecosystem to the atmosphere. Studies of ecosystem production during succession have

typically used the ecological sign convention (e.g., Chapin *et al.*, 2002), whereas most recent studies of half-hour whole-ecosystem flux have used the atmospheric sign convention (e.g., Baldocchi, 2008).

Results

Species composition and LAI

The 1- to 15-year-old stands were dominated by small resprouting shrubs and herbaceous ruderals, with tree species present only as seedlings (Table 1). The 23- and 40-year-old stands were dominated by jack pine, aspen, and black spruce saplings, with small patches of sphagnum (*Sphagnum* spp.) and feathermoss (*Pleurozium* or *Hylocomium* spp.). The 74- and 154-year-old stands were closed-canopy black spruce forest with a thick, continuous layer of sphagnum and feathermoss.

The LAI at the UCI sites increased rapidly from $0.3\,m^2\,m^{-2}$ 1 year after the burn to $2.1\,m^2\,m^{-2}$ 6 years after burn to $5.5\,m^2\,m^{-2}$ 23 years after burn (Fig. 3). LAI plateaued at 5.3–5.5 $m^2\,m^{-2}$ from 23 to 154 years, except for a peak of $7.2\,m^2\,m^{-2}$ at the 74-year-old site. The relative importance of deciduous and evergreen plants shifted during succession, with deciduous herbs (grass and fireweed) and shrubs (alder and willow) assuming initial importance, and evergreens (black spruce and moss) dominating older sites.

NPP

Vascular plant ANPP at the UCI sites increased rapidly, rising from $12\,g\,C\,m^{-2}\,yr^{-1}$ at the 1-year-old stand to $70\,g\,C\,m^{-2}\,yr^{-1}$ at the 6-year-old stand (Fig. 4a). Vascular ANPP peaked at $243\,g\,C\,m^{-2}\,yr^{-1}$ at the 23-year-old stand and declined to $126\,g\,C\,m^{-2}\,yr^{-1}$ at the 154-year-old stand. Vascular ANPP was similar between the UCI and UW sites, with the exception of the 40-year-old burn, where the UW stand was much more productive (Fig. 4a).

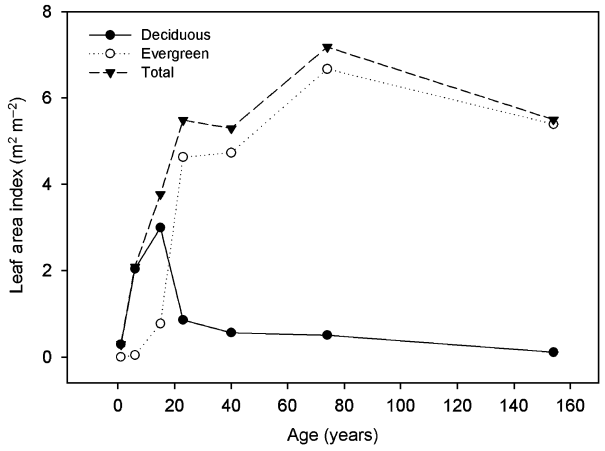

Fig. 3 Deciduous (filled circles), evergreen (unfilled circles), and total (filled triangles) leaf area index (LAI, $m^2\,m^{-2}$) during the late growing season (August 2004) as a function of time since last burn.

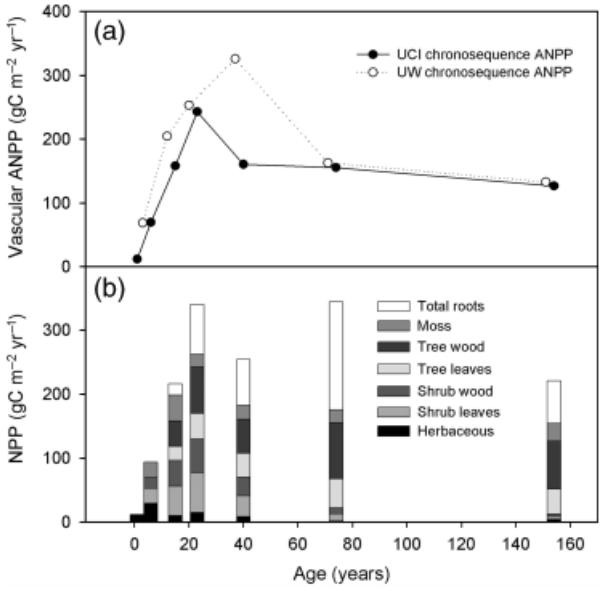

Fig. 4 (a) Comparison of vascular plant aboveground net primary production (ANPP, $g\,C\,m^{-2}\,yr^{-1}$; excludes moss and belowground production) at the UCI sites (filled circles) and the UW sites (open circles) as a function of time since last burn. (b) Components of total NPP as a function of time since last burn. Aboveground vascular production (herbaceous plants, shrubs, and trees) was measured at the UCI sites in late 2004. Moss production was measured at the UCI sites in 2004. Root production was measured at the UW sites in 2001 (data from Bond-Lamberty *et al.*, 2004). Root production observations were unavailable for the 1-year-old stand and were considered unreliable for the 6-year-old stand.

The distribution of production by plant functional type (Fig. 4b) paralleled the changes in LAI and species composition (Fig. 3; Table 1). Production at the younger stands was dominated by shrubs and herbaceous plants; production at the older stands was dominated by trees.

BNPP was greatest at the 74-year-old stand and somewhat reduced at the 23-, 40-, and 154-year-old stands (Total roots in Fig. 4b). BNPP was always less than ANPP. Some of the BNPP differences between stands may reflect sampling variability (Table 3; Bond-Lamberty *et al.*, 2004). BNPP measurements were unavailable for the 1-year-old stand and were considered unreliable at the 6-year-old stand. Many of the plants at the 6-year-old stand were geophytes or cryptophytes, which store carbohydrates in their roots or rhizomes

during winter. These belowground stores were not well sampled by the max–min coring approach, which assumes root production and stocks are greatest in mid-summer.

TNPP peaked at the 23- and 74-year-old stands, declined at the 154-year-old stand, and was somewhat reduced at the 40-year-old stand (Fig. 4b). The dip at the 40-year-old stand may have been due in part to uncertainty and variability in the measurements of belowground production, and also to possible mismatches in site selection (see 'Discussion').

Biomass and carbon stocks

Live biomass (vascular plants and bryophytes) increased from $12\,g\,C\,m^{-2}$ at the 1-year-old stand to $5680\,g\,C\,m^{-2}$ in the 154-year-old stand (Fig. 5). The stand-to-stand biomass increment was comparatively low among the youngest and among the oldest stands and high between the 40- and 74-year-old stands. The initial acceleration in biomass accumulation (Fig. 5) paralleled the observed increases in ANPP and allocation to long-lived tissues such as wood (Fig. 4). The net biomass increment between the youngest two sites ($17\,g\,C\,m^{-2}\,yr^{-1}$) was similar to the ANPP of long-lived tissues at the 6-year-old stand ($17\,g\,C\,m^{-2}\,yr^{-1}$). The net increment between the 15- and 23-year-old stands ($75\,g\,C\,m^{-2}\,yr^{-1}$) was less than the ANPP of long-lived tissues at the 23-year-old stand ($166\,g\,C\,m^{-2}\,yr^{-1}$).

Carbon stocks in the forest floor ($C_{forest\ floor}$) were comparatively high in the 1-year-old stand, low in the 6-, 15-, 23-, and 40-year-old stands, and very high in the 74- and 154-year-old stands. C_{CWD} were broadly constant across sites, with somewhat greater stocks at the 6-, 23-, and 40-year-old stands and lower stocks at the 74-year-old stand. $C_{forest\ floor}$ was more dynamic than C_{CWD}; $C_{forest\ floor}$ ranged by $3200\,g\,C\,m^{-2}$ between stands, while C_{CWD} ranged by $800\,g\,C\,m^{-2}$. $C_{forest\ floor}$ and C_{CWD} followed nearly opposite trajectories, with $C_{forest\ floor}$ increasing markedly and C_{CWD} decreasing between the 40- and 74-year-old stands.

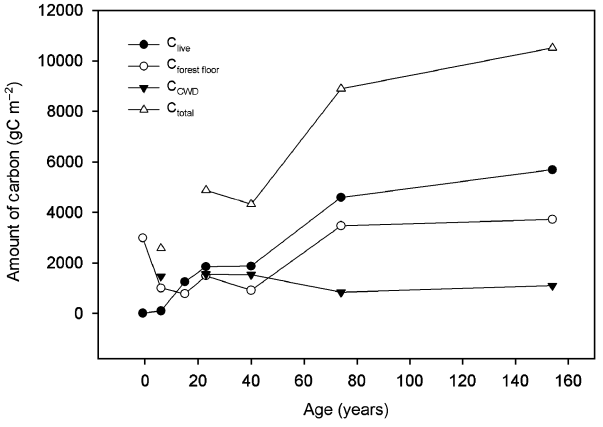

Fig. 5 Live plant carbon stocks (C_{live}; filled circles, $g\,C\,m^{-2}$) calculated as the sum of vascular biomass and moss biomass at the UCI sites. Forest floor carbon stocks ($C_{forest\ floor}$; open circles, $g\,C\,m^{-2}$) at the UCI sites. Coarse woody debris carbon stocks (C_{CWD}; filled triangles, $g\,C\,m^{-2}$) at the UCI sites (data from Manies *et al.*, 2005). Total carbon stocks (C_{total}, $g\,C\,m^{-2}$) calculated as the sum of C_{live}, $C_{forest\ floor}$, and C_{CWD}. C_{CWD} and C_{total} were unavailable for the 1- and 15-year-old stands.

The sum of live biomass, forest floor, and CWD provides a measure of total carbon (C_{total}), which can be used to calculate NEP based on changes in stocks (NEP_{stocks}; Table 2) if we assume the amount of carbon in the soil beneath the forest floor is static (Trumbore & Harden, 1997; Wang *et al.*, 2003). Total carbon was comparatively constant among the 15-, 23-, and 40-year-old stands and also among the 74- and 154-year-old stands. Total carbon increased considerably between the 40- and 74-year-old stands (Fig. 5), reflecting the accumulation of carbon in live plants and the forest floor.

GPP and respiration

The peak rate of mid-day CO_2 uptake was remarkably consistent at all sites except the 1-year-old burn (Fig. 6). Peak CO_2 uptake was not related solely to either LAI or leaf longevity; the 6-year-old stand, which had a deciduous canopy with an LAI of $2.1\,m^2\,m^{-2}$, and the 74-year-old stand, which had an evergreen canopy with an LAI of $7.2\,m^2\,m^{-2}$, both had a maximum CO_2 uptake of $10\,\mu mol\,m^{-2}\,s^{-1}$ (see also McMillan & Goulden, 2008).

The growing season length and seasonal patterns of NEE mirrored the shifts in leaf phenology (Fig. 3). The 2004 growing season length, calculated as the period when the maximum daily uptake was at least 35% of the maximum summer NEE (McMillan *et al.*, 2008), lasted 68 days at the 6-year-old stand and 88 days at the 15-year-old stand. The 2004 growing season was 126 days at the 23-year-old stand, 138 days at the 40-year-old stand, 137 days at the 74-year-old stand, and 146 days at the 154-year-old stand. The youngest two stands were dominated by deciduous plants and had comparatively short growing seasons; the oldest four stands were dominated by evergreens and had long growing seasons.

The trends in GPP with age followed the shifts in growing season length (Fig. 6). Average GPP increased from $380\,g\,C\,m^{-2}\,yr^{-1}$ at the 6-year-old stand to $450\,g\,C\,m^{-2}\,yr^{-1}$ at the 15-year-old stand to $710\,g\,C\,m^{-2}\,yr^{-1}$ at the 23-year-old stand (Fig. 7). GPP ranged from 630 to $720\,g\,C\,m^{-2}\,yr^{-1}$ at the three oldest stands. The increase in GPP from the 15- to 23-year-old

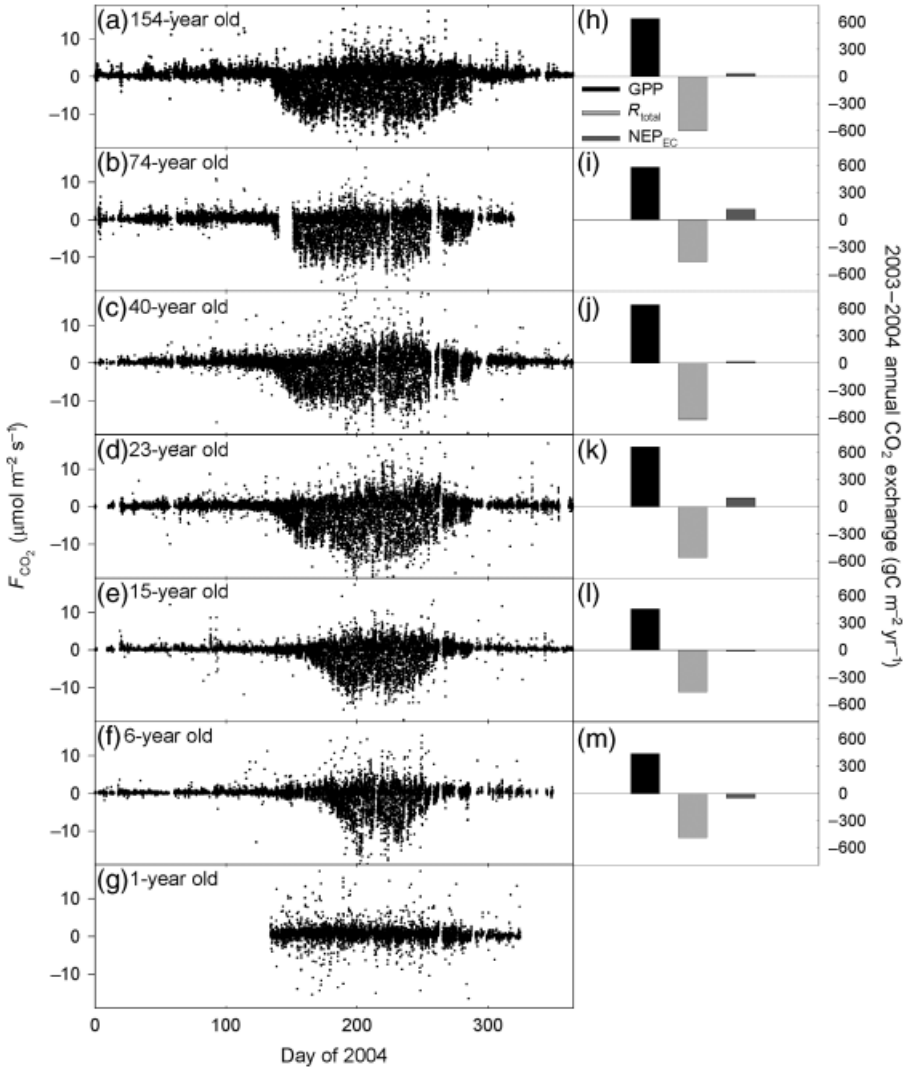

Fig. 6 (a–g) Net CO_2 exchange (F_{CO_2}; 30 min covariances, μmol m^{-2} s^{-1}) during 2004 at seven sites that differ in age since last burn. (h–m) Gross primary production (GPP, g C m^{-2} yr^{-1}), ecosystem respiration (R_{total}, g C m^{-2} yr^{-1}), and net ecosystem production (NEP_{EC}, g C m^{-2} yr^{-1}) integrated from October 1, 2003 to September 30, 2004 at the six sites with year-round observations. F_{CO_2} is presented in the atmospheric sign convention, with a positive flux indicating the net transfer of carbon from the ecosystem to the atmosphere. GPP, R_{total}, and NEP_{EC} are presented in the ecological sign convention, with a positive flux indicating the net transfer of carbon from the atmosphere to the ecosystem.

stand coincided with the transition from mainly deciduous to mainly evergreen vegetation (Fig. 3) and the associated increase in growing season length.

Whole ecosystem respiration (R_{total}) was comparatively high at the 23-, 45-, and 154-year-old stands (Fig. 7). The site-to-site patterns of R_{total} broadly paralleled the patterns of GPP. The higher rate of R_{total} at the 23- and 45-year-old stands coincided with comparatively high rates of GPP. The maximum rates of both R_{total} and GPP were observed at the 154-year-old stand. R_{total} was more consistent between stands than was GPP; R_{total} ranged by 230 g C m^{-2} yr^{-1} between sites whereas GPP ranged by 340 g C m^{-2} yr^{-1}.

NEP

The annually integrated net CO_2 exchange (NEP_{EC}; Fig. 8) indicated the 1- and 6-year-old stands were losing carbon, the 15-year-old stand was gaining a small amount of carbon, the 23- and 74-year-old stands were gaining considerable carbon, and the 40- and 154-year-old stands were gaining modest amounts of carbon. A linear fit through all the NEP_{EC} observations at the 6- and 15-year-old stands indicated the transition from carbon source to sink occurred at an age of 11–12 years. NEP_{EC} was variable among the four oldest sites, with consistently high rates of carbon storage at the 23- and

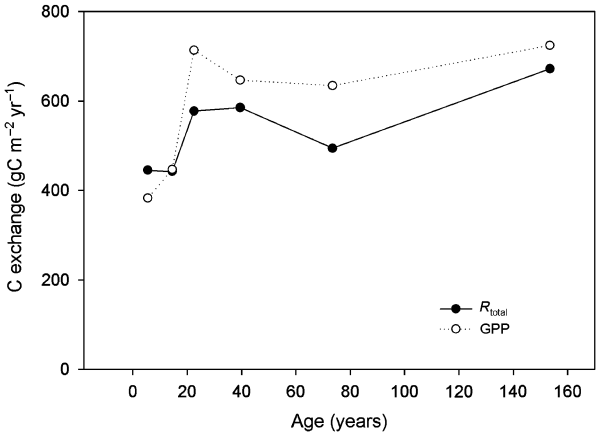

Fig. 7 Gross primary production (GPP; unfilled circles, $g C m^{-2} yr^{-1}$) and total respiration (R_{total}; filled circles, $g C m^{-2} yr^{-1}$) averaged across 2002–03 and 2003–04 as a function of time since last burn.

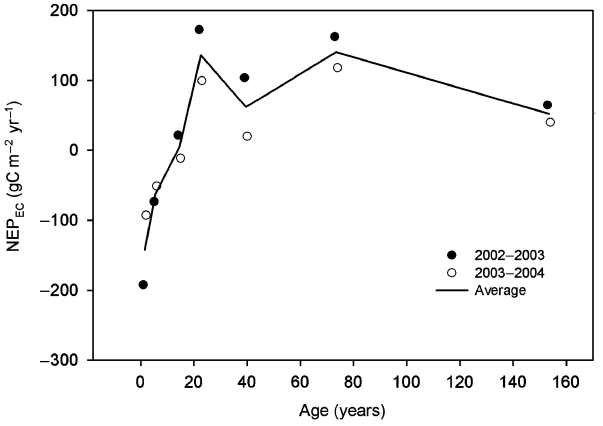

Fig. 8 Net ecosystem production (NEP_{EC}, $g C m^{-2} yr^{-1}$) as a function of time since last burn. Points show annual integrals for 2002–03 (filled circles), 2003–04 (open circles), and the 2002–04 average (solid line). NEP_{EC} is presented in the ecological sign convention, with a positive flux indicating the net transfer of carbon from the atmosphere to the ecosystem.

74-year-old stands and low rates at the 40- and 154-year-old stands (see also McMillan *et al.*, 2008). The comparatively high rates of NEP_{EC} at the 23-year-old stand (Fig. 8) coincided with high rates of GPP (Fig. 7), whereas the high rates of NEP_{EC} at the 74-year-old stand coincided with reduced R_{total}.

UCIs 154-year-old stand was 400 m from the BOREAS NSA NOBS eddy covariance tower (Table 1; NOBS-1850), which began operation in 1995 (Goulden *et al.*, 1997; Dunn *et al.*, 2007). The NEP_{EC}s at NOBS-1850 and UCI-1850 were comparable, with similar patterns of interannual variability (Table 4). The long-term record at NOBS-1850 indicates a marked increase in NEP around 1998–2000. NEP_{EC} at NOBS-1850 averaged $40 g C m^{-2} yr^{-1}$ in 2003–04 and $2 g C m^{-2} yr^{-1}$ in 1995–2004 (Table 4). The cause of this trend is not fully understood, though it may be related to water table depth (Dunn *et al.*, 2007).

Discussion

Comparison of integrated eddy covariance with biomass accumulation

The suite of measurements allowed us to calculate NEP along the chronosequence using three fully independent approaches (Table 2): (1) integrated eddy covariance (NEP_{EC}; Fig. 8), (2) site-to-site differences in total carbon stocks (NEP_{stocks}; Fig. 5), and (3) NPP minus decomposition estimated from soil and woody debris respiration (NEP_{NPP}; Bond-Lamberty *et al.*, 2004). The three approaches gave broadly similar results (Fig. 9), with a loss of carbon that lasted $\sim$ 10 years and peaked at 50–150 $g C m^{-2} yr^{-1}$, followed by an extended period of net carbon uptake of 50–150 $g C m^{-2} yr^{-1}$ from $\sim$10 to 100 years, and a reduced net carbon uptake of 0–50 $g C m^{-2} yr^{-1}$ after $\sim$100 years. The NEP_{stocks} approach was comparatively variable over time, which likely reflects spatial heterogeneity and landscape scale sampling uncertainty (Table 3). Unfortunately, C_{CWD} observations were unavailable for the 1-year-old site, and we were unable to determine the changes in C_{total} during the first few years after fire.

A more quantitative comparison of methods is possible by considering the long-term rates of carbon sequestration. The difference in C_{total} between the 6- and 74-year-old stands was 6500 $g C m^{-2}$ (Fig. 5), whereas the integrated NEP_{EC} between these stands was 5400 $g C m^{-2}$ (Fig. 8). The difference in C_{total} between the 6- and 154-year-old stands was 8400 $g C m^{-2}$, whereas the integrated NEP_{EC} between these stands was 13 000 $g C m^{-2}$. The calculation of integrated NEP_{EC} between the 6- and 154-year-old stands may be confounded by the wide age difference between the oldest stands and uncertainty over how long the high NEP_{EC} observed at the 74-year-old stand continues. Additionally, integrated NEP_{EC} may have overestimated long-term carbon storage as a result of temporal sampling error (Table 3). The observations at NOBS-1850 indicate the carbon uptake during 2003–2004 was $\sim 40 g C m^{-2} yr^{-1}$ greater than during 1995–2004 (Table 4). Tree rings indicate this trend may have occurred at the 74-year-old stand as well (Rocha *et al.*, 2006), suggesting our study period was anomalous. This possibility is consistent with the observation that NEP_{EC} exceeded NEP_{NPP} and NEP_{stocks} in the oldest two stands (Fig. 9). The integrated NEP_{EC} between the 6- and 154-year-old stands after subtracting

Table 4 Eddy covariance NEPs (NEP_{EC}; $g\,C\,m^{-2}\,yr^{-1}$)

	Site							
Year	UCI-2003	UCI-1998	UCI-1989	UCI-1981	UCI-1964	UCI-1930	NOBS-1850	UCI-1850
1995							−41	
1996							−84	
1997							−39	
1998							7	
1999							7	
2000							3	
2001							23	
2002				86	38	174	27	
2003		−73	21	172	104	162	58	64
2004	−192	−52	−12	99	20	118	21	39
2005	−93	−11	32	110	28	184		76

UCI, University of California, Irvine.

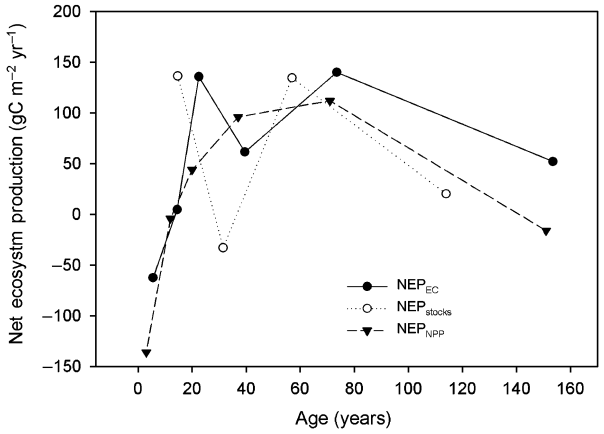

Fig. 9 Net ecosystem production (NEP, $g\,C\,m^{-2}\,yr^{-1}$) calculated by integrated eddy covariance (NEP_{EC}; filled circles; data from Fig. 8), site-to-site changes in total carbon stocks (NEP_{stocks}; unfilled markers; calculated from C_{total} in Fig. 5), and NPP minus decomposition (NEP_{NPP}; filled triangles; data from Bond-Lamberty *et al*., 2004) as a function of time since last burn.

$40\,g\,C\,m^{-2}\,yr^{-1}$ at the 74- and 154-year-old stands was $9200\,g\,C\,m^{-2}$. Given the variety and range of uncertainties (Table 3), the agreement between the measures of NEP is quite reasonable.

Sampling challenges

Landscape heterogeneity, both between and within fires, is a poorly characterized and potentially large source of uncertainty in chronosequence studies (referred to as across landscape sampling accuracy in Table 3). The UCI chronosequence appeared well matched with the notable exception of the 40-year-old stand, where a variety of measures indicate anomalously low productivity. TNPP, C_{live}, and NEP_{EC} were less at the 40-year-old stand than would be expected based on the 23- and 74-year-old stands (Figs 4, 5 and 8). Likewise, vascular plant ANPP at the UCI sites was generally similar to that at the UW sites except for UCI-1964, which was much less productive than UW-D1964 (Fig. 4a). A 6-week record of eddy covariance measurements for an area near UW-D1964 (Litvak *et al*., 2003) suggests a much higher NEP_{EC} than at UCI-1964. A possible discrepancy at UCIs 40-year-old stand was also identified in remote sensing analyses, which indicated lower enhanced vegetation indices (EVI) at UCI-1964 than other comparably aged stands (Goulden *et al*., 2006). The EVI analysis also indicated UCI's 23-year-old stand may be somewhat more productive than is typical for the area. The possibility of site-to-site mismatches, especially at the 40-year-old stand, should be considered when interpreting the figures.

Our selection of eddy covariance sites was conducted in 2001 and included visits to several candidates in each burn. In retrospect, the selection process would have benefited from an extensive survey of the spatial variation within each burn using satellite imagery. Satellite analyses during the early phases of site selection and identification would have been particularly useful for objectively identifying representative stands of given ages. However, we were unable to carry out this analysis until late 2005 (Goulden *et al*., 2006), when advances in the availability of MODIS and Landsat imagery, image analysis software, and computing power facilitated the investigation. Vegetation indices and products are available for albedo, LAI, and CO_2 uptake, allowing consideration of several biophysical attributes (McMillan & Goulden, 2008). Incorporation of remote sensing analyses at an early planning stage could have improved the match between sites and should be considered in future chronosequence studies.

Changes in stocks during succession

The hypotheses in Fig. 1 were originally sketched by hand, and were intended as qualitative and relative predictions. Judged against this goal, the models did a good job of capturing the dominant patterns during succession.

The observed changes in biomass and detrital pools matched the predictions particularly well (Figs 1a and 10a), probably because biomass is comparatively easy to measure and these predictions could be based on direct observation (Bormann & Likens, 1979). The observed recovery of C_{live} (Fig. 5) followed the expected logistic pattern, with slow initial accumulation followed by rapid accumulation in mid-succession and reduced accumulation in the oldest stand. The detrital pools also matched the predictions, with both $C_{forest\ floor}$ and C_{CWD} showing comparatively high levels following fire, subsequent declines in early or mid-succession, and increases in late succession. $C_{forest\ floor}$ was more dynamic than C_{CWD}, with larger and more rapid changes in pool size. Unfortunately, measurements of C_{CWD} were unavailable for the 1- and 15-year-old stands, which prevented complete comparison of observed and predicted C_{total}. Nonetheless, it is likely the changes in C_{total} matched the predictions, with initial loss, followed by rapid accumulation, and reduced accumulation in the oldest stand. $C_{forest\ floor}$ was markedly different between the 1- and 6-year-old stands, corresponding to a loss of $430\,g\,C\,m^{-2}\,yr^{-1}$. Wang *et al*. (2003) observed a similar large drop in $C_{forest\ floor}$ between the youngest UW stands. It is likely C_{total} declined considerably during the first 5 years following fire, with most of this loss coming from $C_{forest\ floor}$.

Patterns of NPP, GPP, respiration, and NEP during succession

The observed changes in NEP, NPP, and GPP (Fig. 10b and c) broadly matched the predictions (Fig. 1b and c). NEP_{EC} was initially negative, transitioned to an extended period of carbon accumulation, and showed reduced accumulation in the oldest stand. NPP and GPP were initially low after fire, recovered to a peak in early and mid-succession, and either declined (NPP) or remained constant (GPP) at the oldest stand. The initial suppression of NPP and GPP following disturbance was brief, and the peak rate of NPP was observed at the 23-year-old stand. The TNPP decline at the oldest stand was not as large as expected. The lack of a dramatic decline may simply reflect the range of ages sampled; the rates of production in stands older than 154 years may be lower, though most forest in the area burns before it reaches this age.

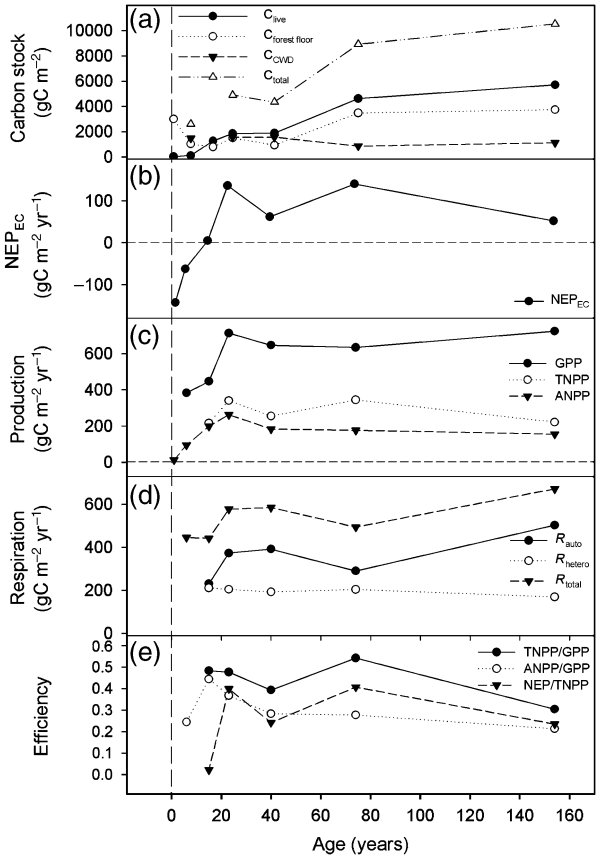

Fig. 10 (a) Live biomass (C_{live}; filled circles; data from Fig. 5), forest floor carbon stocks ($C_{forest\ floor}$; open circles; data from Fig. 5), CWD (C_{CWD}; filled triangles; data from Fig. 5), and total carbon stocks (C_{total}; open triangles; data from Fig. 5) as a function of time since last burn. (b) Net ecosystem production (NEP_{EC}; filled circles; data from Fig. 8). (c) Gross primary production (GPP; filled circles; from Fig. 7), total net primary production (TNPP; open circles; calculated from Fig. 4b), and aboveground net primary production (ANPP; filled triangles; calculated from Fig. 4b; includes moss production). (d) Autotrophic respiration (R_{auto}; filled circles; calculated as the difference between GPP and TNPP), heterotrophic respiration (R_{hetero}; open circles; calculated as the difference between TNPP and NEP_{EC}), and total respiration (R_{total}; filled triangles; from Fig. 7). (e) Total plant production efficiency (TNPP/GPP; filled circles; calculated from Figs 4b and 7), Aboveground primary production efficiency (ANPP/GPP; open circles; calculated from Figs 4b and 7) and ecosystem carbon storage efficiency (NEP/ANPP; open triangles; calculated from Figs 4b and 8). The time of fire is indicated by the dashed vertical line. C_{CWD}, C_{total}, GPP, TNPP, R_{total}, R_{hetero}, R_{auto}, TNPP/GPP, and ANPP/GPP were unavailable for the 1-year-old stand. TNPP, R_{hetero}, R_{auto}, and TNPP/GPP were unavailable for the 6-year-old stand. C_{CWD} and C_{total} were unavailable for the 15-year-old stand.

The observed patterns of respiration (Fig. 10d) did not match the predictions as well (Fig. 1d). R_{auto} was initially low and varied considerably during succession

in a way that paralleled GPP, as predicted. Variation in R_{total} was most strongly driven by variation in R_{auto}, and, as a result, R_{total} peaked in mid-succession and was reduced in the youngest stands, also as predicted. But R_{auto} increased in the oldest stand, at a time when a decrease was predicted. And the changes in R_{hetero} in the youngest or oldest stands were less than predicted. The difficulty of predicting respiration mirrors the general observation that respiration in terrestrial ecosystems is poorly understood relative to photosynthesis (Trumbore, 2006).

Why is the loss of carbon in the decade following disturbance less than expected?

The initial loss of carbon following disturbance (Fig. 10b) was neither as protracted nor large as predicted (Fig. 1b). A similar pattern has been observed in other eddy covariance chronosequence studies of boreal fire recovery, which have reported only modest carbon losses in the decade following disturbance and a transition to annual net uptake within 10–15 years (Litvak *et al*., 2003; Amiro *et al*., 2006; Randerson *et al*., 2006).

This muted response may reflect the rapid regrowth of vegetation following fire. Boreal forests have an extensive community of ruderal and resprouting herbs and shrubs that rapidly reestablish LAI, GPP, and NPP (Figs 3, 4, 6, and 7), and allow a quick transition from carbon source to sink. Other ecosystems may be less well adapted to crown fire. The rapid recovery of midday NEE and annual NEP we observed contrasts with that observed after a crown fire in a southwestern ponderosa pine stand (Dore *et al*., 2008). We found the mid-season daytime rates of CO_2 uptake had recovered to the rates observed in older stands, and the annual NEP approached zero, within 10 years after fire (Fig. 6). In contrast, Dore *et al*. (2008) found the mid-season daytime rates of CO_2 uptake were less than half those observed in an older stand, and the site was still a large source of CO_2, 10 years after fire. Southwestern US pine forests were historically exposed to frequent low-intensity ground fires, and, as a result, lack a plant community that is adapted for swift tree establishment and regrowth following crown fire (Savage & Mast, 2005).

Boreal fires consume most of the fine fuel, while killing the trees and leaving coarse woody debris standing. Standing debris takes a long time to decompose (Yatskov *et al*., 2003; Bond-Lamberty & Gower, 2008), and the relative lack of fine detritus may also help explain the muted NEP response. The annual carbon loss in the first years after disturbance normalized by the maximum uptake during regrowth may differ between forests recovering from clear cut and those recovering from crown fire. The annual carbon loss observed 2–3 years after clear cutting in a boreal pine forest (Zha *et al*., 2009) and also in a Douglas fir forest (Humphreys *et al*., 2006) was roughly twice the annual peak uptake observed for older but otherwise comparable stands. In contrast, we estimated a peak efflux 2–3 years after fire that was $<70\%$ of the peak uptake observed for older stands (Fig. 8). This pattern is consistent with a difference in the input of fine and coarse debris during disturbance. Clear cutting leaves large amounts of fine slash, which would be expected to decompose rapidly, resulting in a high peak efflux. Crown fire leaves mostly coarse and standing debris, which would be expected to decompose slowly, resulting in a muted efflux.

Why does NPP decline in older stands?

The cause of reduced NPP in old stands has been the subject of considerable interest (Ryan *et al*., 1997), with a variety of mechanisms proposed, including ones that posit NPP/GPP is constant and attribute declining NPP to declining GPP, and ones that posit NPP/GPP varies and attribute declining NPP to increasing R_{auto}. Our findings at the 154-year-old stand contradict the idea that NPP/GPP is constant (Fig. 1e), and are most consistent with mechanisms involving increasing R_{auto}. GPP increased slightly from the 23- to 154-year-old stand, while TNPP decreased by 35% and ANPP decreased by 41%. These trends resulted in a large decrease in biomass production efficiency (Fig. 10e); TNPP/GPP decreased from 0.47 at the 23-year-old stand to 0.31 at the 154-year-old stand, and ANPP/GPP decreased from 0.36 at the 23-year-old stand to 0.21 at the 154-year-old stand. Our observations support previous reports that old growth forest often has a low NPP/GPP (e.g. Kira, 1975; Amthor & Baldocchi, 2001; Chambers *et al*., 2004; Delucia *et al*., 2007; Figueira *et al*., 2008).

We were unable to directly identify the physiological basis for increasing R_{auto} in the 154-year-old stand. The increase in R_{auto} did not appear to be caused by accelerated maintenance respiration with increased biomass (e.g., Waring & Schlesinger, 1985). R_{auto} did not vary with age in direct proportion to C_{live}; the biggest change in C_{live} occurred from the 23- and 40-year-old stands to the 74-year-old stand (Fig. 5), a period when R_{auto} decreased or remained constant (Fig. 10). Likewise, the increase in R_{auto} at the 154-year-old stand does not appear to be caused by increased growth respiration, since this trend coincided with declining ANPP and TNPP (Fig. 10).

A more plausible explanation involves increasing allocation to fine root turnover, root metabolism,

alternative forms of respiration, mycorrhizal relationships, or root exudation, possibly caused by progressive nutrient limitation. Boreal forests are thought to experience nutrient limitation with age, as a result of sequestration in detritus and soil cooling by moss and the evergreen canopy (Van Cleve *et al*., 1983; Bonan & Shugart, 1989). Unfortunately, we lack detailed direct observations of the patterns of belowground and respiratory allocation during succession. The observations of root production are somewhat erratic from site-to-site as a result of sampling challenges (Fig. 4; Table 3), and more information on belowground allocation and production is needed (Gower *et al*., 2001). Nonetheless, the existing data are consistent with increasing allocation belowground over time. The fraction of GPP allocated to root NPP (Figs 4b and 7) was lowest in the 15-year-old stand (4%), moderate in the 23-, 40- and 154-year-old stands (9–11%) and greatest in the 74-year-old stand (27%).

Carbon accumulation by old stands

We found high rates of carbon accumulation at the 74-year-old stand and reduced carbon accumulation at the 154-year-old stand (Figs 9 and 10). The transition between the 40- and 74-year-old stands was marked by the closure of the black spruce canopy and the establishment of a continuous moss layer (Table 1). Black spruce trees are relatively long lived, with a life span of up to ~200 years (Viereck & Johnston, 1990). Likewise, dead moss is slow to decompose, with a turnover time of ~100 years (Trumbore & Harden, 1997). The high NEP and NEP/TNPP (Fig. 10e) at the 74-year-old stand was a consequence of increased allocation of NPP to black spruce and moss (Fig. 4), which are both relatively long-lived pools. The production of wood caused a large input to and buildup of C_{live}; the production of moss and evergreen needles caused a large input to and buildup of $C_{forest\ floor}$. The buildup of C_{live} and $C_{forest\ floor}$ at the 74-year-old stand resulted in a comparatively high NEP_{EC}.

Both NEP_{EC} and NEP_{stocks} were reduced at the 154-year-old stand relative to the 74-year-old stand (Figs 9 and 10). Moreover, the long-term observations at NOBS-1850 indicate the 154-year-old stand was in approximate steady state with the atmosphere, with a decadal average NEP_{EC} close to zero (Table 4; Dunn *et al*., 2007). The reduced carbon sequestration at the 154-year-old stand did not reflect a decrease in the production of black spruce or moss; these components of production were similar between the 74- and 154-year-old stands (Fig. 4b). Rather, the declines in NEP_{EC}, NEP_{stocks}, and NEP/TNPP imply an increase in the loss from C_{live} by tree mortality and an increase in the loss from $C_{forest\ floor}$ by decomposition. The wood NPP at the 74-year-old stand was $87\,g\,C\,m^{-2}\,yr^{-1}$ (Fig. 4b) whereas the net C_{live} increment between the 40- and 74-year-old stands was $80\,g\,C\,m^{-2}\,yr^{-1}$ (Fig. 5), implying a small loss of C_{live} by mortality. In contrast, the wood NPP at the 154-year-old stand was $75\,g\,C\,m^{-2}\,yr^{-1}$ whereas the net C_{live} increment between the 74- and 154-year-old stands was only $14\,g\,C\,m^{-2}\,yr^{-1}$, implying greater mortality losses. Likewise, the moss and needle production at the 74-year-old stand was $65\,g\,C\,m^{-2}\,yr^{-1}$ whereas the net $C_{forest\ floor}$ increment between the 40- and 74-year-old stands was $74\,g\,C\,m^{-2}\,yr^{-1}$, implying that $C_{forest\ floor}$ decomposition was quite low. In contrast, the moss and tree leaf production at the 154-year-old stand was $66\,g\,C\,m^{-2}\,yr^{-1}$ whereas the net $C_{forest\ floor}$ increment between the 74- and 154-year-old stands was just $6\,g\,C\,m^{-2}\,yr^{-1}$, implying increased decomposition of $C_{forest\ floor}$. This apparent increase in $C_{forest\ floor}$ decomposition was not evident in the patterns of R_{hetero} (Fig. 10d), though this may simply reflect measurement uncertainties (Table 3).

The cause of increased C_{live} mortality and $C_{forest\ floor}$ decomposition losses at the 154-year-old stand is unclear, though it does not appear to be driven exclusively by simple first-order kinetics, where an increase in the size of a homogenous pool accelerates the loss from that pool simply because there is more carbon to die or decay. The rates of mortality and decomposition increased several fold between the 74- and 154-year-old stands, whereas the amounts of $C_{forest\ floor}$ and C_{live} increased by just 15–25% (Fig. 5). Nonetheless, the NEP and carbon storage efficiency (NEP/TNPP) observations support the hypothesis that old stands approach steady state (Fig. 1b and e; Odum, 1969), and are inconsistent with the notion that older forest stands continue to sequester large amounts of carbon (Luyssaert *et al*., 2008).

Implications and conclusions

The strategy of using multiple methods, including biometry and micrometeorology, worked well; in particular, the three independent measures of NEP during succession gave similar results. Nonetheless, landscape heterogeneity, both between and within fires, remains a poorly characterized and potentially large source of uncertainty. Incorporation of remote sensing analyses may help in the selection of sites and the identification of spatial sampling errors. Additionally, a stratified and tiered approach to deploying eddy covariance systems that combines many lightweight and portable towers with a few permanent ones is likely to maximize the science return for a fixed investment.

The existing conceptual models did a good job of capturing the dominant patterns of NPP, GPP, and NEP during succession. The NEP and carbon storage efficiency (NEP/TNPP) observations support the hypothesis that old stands approach steady state. The initial loss of carbon following disturbance was neither as protracted nor large as predicted. This muted response reflects both the rapid regrowth of vegetation following fire and the prevalence of standing coarse woody debris following the fire, which is thought to decay slowly. In general, the patterns of forest recovery from disturbance should be expected to vary as a function of climate, ecosystem type, disturbance intensity, and disturbance type. Future efforts should be directed at understanding how recovery differs between contrasting types of ecosystems, and between different intensities and types of disturbance.

The NPP decline at the older stands appears related to increased R_{auto} rather than decreased GPP. The increase in R_{auto} in the older stands does not appear to be caused by accelerated maintenance respiration with increased biomass, and more likely involves increased allocation to fine root turnover, root metabolism, alternative forms of respiration, mycorrhizal relationships, or root exudates, possibly associated with progressive nutrient limitation. The importance of R_{auto} rather than GPP in controlling mature stand NPP implies that the production of older stands is not limited by carbohydrate availability. If true, this suggests production and carbon storage by older stands may not accelerate with elevated atmospheric CO_2 concentration.

Studies such as this are producing a wealth of information on the patterns of ecosystem function during succession. Process-based models of land–atmosphere exchange are needed to translate this information into a more quantitative understanding of the effects of past disturbance on the contemporary carbon cycle, and also into more reliable predictions of the future climate forcing associated with changes in disturbance regime. Some of the patterns we observed, and the processes we identified as especially important, are poorly represented in many models. We hope researchers who are developing and using process-based models will make use of these observations (see Supporting Information), both to test their models and to identify which processes require particular attention.

Acknowledgements

We thank Scott Miller, Marcy Litvak, Steve Beaupre, Sami Rifai, Anders Holmberg, Aaron Fellows, Kelsey McDuffee, Ruth Errington, and Lee Pruett for help in the lab or field. We thank Thompson Technologies, the NASA Terrestrial Ecology program, and the BOREAS science and support teams for setting up and operating NOBS. We thank Custom Storage, the Northern Lights Bed and Breakfast, the Churchill River Lodge, and Brad and Tara Ritchey for support, space and friendship. We thank Sue Trumbore, Steve Wofsy, Ali Dunn, Tom Gower, Brian Amiro, Marcy Litvak, and especially Hugo Veldhuis for sharing their understanding of the boreal forest. We thank Nisichawayasihk Cree Nation and the Canadian Government for permission to use their land. This work was supported by grants from the National Science Foundation, the Department of Energy, and the Comer Foundation.

References

Amiro BD, Barr AG, Black TA *et al.* (2006) Carbon, energy and water fluxes at mature and disturbed forest sites, Saskatchewan, Canada. *Agricultural and Forest Meteorology*, **136**, 237–251.

Amthor JS, Baldocchi DD (2001) Terrestrial higher plant respiration and net primary production. In: *Terrestrial Global Productivity* (eds Roy J, Saugier B, Mooney HA), pp. 33–59. Academic Press, San Diego.

Baldocchi D (2008) Breathing of the terrestrial biosphere: lessons learned from a global network of carbon dioxide flux measurement systems. *Australian Journal of Botany*, **56**, 1–26.

Bonan GB, Shugart HH (1989) Environmental factors and ecological processes in boreal forests. *Annual Review of Ecology and Systematics*, **20**, 1–28.

Bond-Lamberty B, Gower ST (2008) Decomposition and fragmentation of coarse woody debris: re-visiting a boreal black spruce chronosequence. *Ecosystems*, **11**, 831–840.

Bond-Lamberty B, Wang C, Gower ST (2002a) Aboveground and belowground biomass and sapwood area allometric equations for six boreal tree species of northern Manitoba. *Canadian Journal of Forest Research-Revue Canadienne De Recherche Forestiere*, **32**, 1441–1450.

Bond-Lamberty B, Wang C, Gower ST, Norman J (2002b) Leaf area dynamics of a boreal black spruce fire chronosequence. *Tree Physiology*, **22**, 993–1001.

Bond-Lamberty B, Wang CK, Gower ST (2004) Net primary production and net ecosystem production of a boreal black spruce wildfire chronosequence. *Global Change Biology*, **10**, 473–487.

Bormann F, Likens GE (1979) *Pattern and Process in a Forested Ecosystem: Disturbance, Development, and the Steady State Based on the Hubbard Brook Ecosystem Study.* Springer-Verlag, New York.

Callaghan TV, Collins NJ, Callaghan CH (1978) Photosynthesis, growth and reproduction of *Hylocomium splendens* and *Polytrichum commune* in Swedish Lapland – strategies of growth and population-dynamics of tundra plants. *Oikos*, **31**, 73–88.

Chambers JQ, Tribuzy ES, Toledo LC *et al.* (2004) Respiration from a tropical forest ecosystem: partitioning of sources and low carbon use efficiency. *Ecological Applications*, **14**, S72–S88.

Chapin FS, Matson PA, Mooney HA (2002) *Principles of Terrestrial Ecosystem Ecology.* Springer, New York.

Clark KL, Gholz HL, Castro MS (2004) Carbon dynamics along a chronosequence of slash pine plantations in north Florida. *Ecological Applications*, **14**, 1154–1171.

Clements FE (1916) *Plant succession: an analysis of the development of vegetation.* Carnegie Insitution of Washington, Washington, 512 pp.

Clymo RS (1970) The growth of sphagnum: methods of measurement. *Journal of Ecology*, **58**, 13–49.

Connell JH, Slatyer RO (1977) Mechanisms of succession in natural communities and their role in community stability and organization. *American Naturalist*, **111**, 1119–1144.

Covington WW (1981) Changes in forest floor organic-matter and nutrient content following clear cutting in northern hardwoods. *Ecology*, **62**, 41–48.

Delucia EH, Drake JE, Thomas RB, Gonzalez-Meler M (2007) Forest carbon use efficiency: is respiration a constant fraction of gross primary production? *Global Change Biology*, **13**, 1157–1167.

Dore S, Kolb TE, Montes-Helu M *et al.* (2008) Long-term impact of a stand-replacing fire on ecosystem CO_2 exchange of a ponderosa pine forest. *Global Change Biology*, **14**, 1801–1820.

Dunn AL, Barford CC, Wofsy SC, Goulden ML, Daube BC (2007) A long-term record of carbon exchange in a boreal black spruce forest: means, responses to interannual variability, and decadal trends. *Global Change Biology*, **13**, 577–590.

Falge E, Baldocchi D, Olson R *et al*. (2001) Gap filling strategies for defensible annual sums of net ecosystem exchange. *Agricultural and Forest Meteorology*, **107**, 43–69.

Figueira A, Miller SD, De Sousa CAD, Menton MC, Maia AR, Da Rocha HR, Goulden ML (2008) Effects of selective logging on tropical forest tree growth. *Journal of Geophysical Research-Biogeosciences*, **113**, G00B05, doi: 10.1029/2007JG000577.

Finnigan J (2008) An introduction to flux measurements in difficult conditions. *Ecological Applications*, **18**, 1340–1350.

Goulden ML, Daube BC, Fan SM, Sutton DJ, Bazzaz A, Munger JW, Wofsy SC (1997) Physiological responses of a black spruce forest to weather. *Journal of Geophysical Research-Atmospheres*, **102**, 28987–28996.

Goulden ML, Munger JW, Fan SM, Daube BC, Wofsy SC (1996) Measurements of carbon sequestration by long-term eddy covariance: methods and a critical evaluation of accuracy. *Global Change Biology*, **2**, 169–182.

Goulden ML, Winston GC, McMillan AMS, Litvak ME, Read EL, Rocha AV, Elliot JR (2006) An eddy covariance mesonet to measure the effect of forest age on land–atmosphere exchange. *Global Change Biology*, **12**, 2146–2162.

Gower ST, Krankina O, Olson RJ, Apps M, Linder S, Wang C (2001) Net primary production and carbon allocation patterns of boreal forest ecosystems. *Ecological Applications*, **11**, 1395–1411.

Harden JW, O'Neill KP, Trumbore SE, Veldhuis H, Stocks BJ (1997) Moss and soil contributions to the annual net carbon flux of a maturing boreal forest. *Journal of Geophysical Research-Atmospheres*, **102**, 28805–28816.

Harden JW, Munster J, Manies KL, Mack MC, Bubier JL (2009) *Changes in species, areal cover, and production of moss across a fire chronosequence in Interior Alaska*. US Geological Survey Open File Report, 2009-1208.

Houghton RA, Hobbie JE, Melillo JM, Moore B, Peterson BJ, Shaver GR, Woodwell GM (1983) Changes in the carbon content of terrestrial biota and soils between 1860 and 1980 – a net release of CO_2 to the atmosphere. *Ecological Monographs*, **53**, 235–262.

Humphreys ER, Black TA, Morgenstern K, Cai TB, Drewitt GB, Nesic Z, Trofymow JA (2006) Carbon dioxide fluxes in coastal Douglas-fir stands at different stages of development after clearcut harvesting. *Agricultural and Forest Meteorology*, **140**, 6–22.

Hurtt GC, Pacala SW, Moorcroft PR, Caspersen J, Shevliakova E, Houghton RA, Moore B (2002) Projecting the future of the US carbon sink. *Proceedings of the National Academy of Sciences of the United States of America*, **99**, 1389–1394.

Kira T (1975) Primary production of forests. In: *Photosynthesis and Productivity in Different Environments, International Biological Programme*, Vol. 3 (ed. Cooper JP), pp. 5–40. Cambridge University Press, London.

Kira T, Shidei T (1967) Primary production and turnover of organic matter in different forest ecosystems of the western Pacific. *Japanese Journal of Ecology*, **17**, 70–87.

Law BE, Sun OJ, Campbell J, Van Tuyl S, Thornton PE (2003) Changes in carbon storage and fluxes in chronosequence of ponderosa pine forest. *Global Change Biology*, **9**, 510–524.

Litvak M, Miller S, Wofsy S, Goulden ML (2003) Effect of stand age on whole ecosystem CO_2 exchange in the Canadian boreal forest. *Journal of Geophysical Research-Atmospheres*, **108**, 8225, doi: 10.1029/2001JD000854.

Luyssaert S, Schulze ED, Borner A *et al*. (2008) Old-growth forests as global carbon sinks. *Nature*, **455**, 213–215.

Mack MC, Treseder KK, Manies KL *et al*. (2008) Recovery of aboveground plant biomass and productivity after fire in mesic and dry black spruce forests of interior Alaska. *Ecosystems*, **11**, 209–225.

Manies KL, Harden JW, Bond-Lamberty BP, O'Neill KP (2005) Woody debris along an upland chronosequence in boreal Manitoba and its impact on long-term carbon storage. *Canadian Journal of Forest Research-Revue Canadienne De Recherche Forestiere*, **35**, 472–482.

Manies KL, Harden JW, Veldhuis H (2006). *Soil data from a moderately well and somewhat poorly drained fire chronosequence near Thompson, Manitoba, Canada*. US Geological Survey Open-File Report 2006-1291. 17 pp.

McMillan A, Goulden M (2008) Age-dependent variation in the biophysical properties of boreal forests. *Global Biogeochemical Cycles*, **22**, GB2019, doi: 10.1029/2007GB003038.

McMillan A, Winston G, Goulden M (2008) Age-dependent response of boreal forest to temperature and rainfall variability. *Global Change Biology*, **14**, 1904–1916.

Mkhabela MS, Amiro BD, Barr AG *et al*. (2009) Comparison of carbon dynamics and water use efficiency following fire and harvesting in Canadian boreal forests. *Agricultural and Forest Meteorology*, **149**, 783–794.

Noormets A, Chen J, Crow TR (2007) Age-dependent changes in ecosystem carbon fluxes in managed forests in northern Wisconsin, USA. *Ecosystems*, **10**, 187–203.

Odum EP (1969) Strategy of ecosystem development. *Science*, **164**, 262–270.

Randerson JT, Liu H, Flanner MG *et al*. (2006) The impact of boreal forest fire on climate warming. *Science*, **314**, 1130–1132.

Reichstein M, Falge E, Baldocchi D *et al*. (2005) On the separation of net ecosystem exchange into assimilation and ecosystem respiration: review and improved algorithm. *Global Change Biology*, **11**, 1424–1439.

Rocha AV, Goulden ML, Dunn AL, Wofsy SC (2006) On linking interannual tree ring variability with observations of whole-forest CO_2 flux. *Global Change Biology*, **12**, 1378–1389.

Ryan MG, Binkley D, Fownes JH (1997) Age-related decline in forest productivity: pattern and process. *Advances in Ecological Research*, **27**, 213–262.

Savage M, Mast JN (2005) How resilient are southwestern ponderosa pine forests after crown fires? *Canadian Journal of Forest Research-Revue Canadienne De Recherche Forestiere*, **35**, 967–977.

Sellers PJ, Hall FG, Kelly RD *et al*. (1997) BOREAS in 1997: experiment overview, scientific results, and future directions. *Journal of Geophysical Research-Atmospheres*, **102**, 28731–28769.

Sprugel DG (1985) Natural disturbance and ecosystem energetic. In: *The Ecology of Natural Disturbance and Patch Dynamics* (eds Pickett S, White P), pp. 335–352. Academic Press, New York.

Trumbore S (2006) Carbon respired by terrestrial ecosystems – recent progress and challenges. *Global Change Biology*, **12**, 141–153.

Trumbore SE, Harden JW (1997) Accumulation and turnover of carbon in organic and mineral soils of the BOREAS northern study area. *Journal of Geophysical Research-Atmospheres*, **102**, 28817–28830.

Van Cleve K, Dyrness CT, Viereck LA, Fox J, Chapin FS, Oechel W (1983) Taiga ecosystems in interior Alaska. *Bioscience*, **33**, 39–44.

Viereck LA, Johnston WF (1990) Black spruce. In: *Silvics of North America*, Vol. 1 (eds Burns RM, Honkala BH), pp. 227–237. USDA-Forest Service, District of Columbia.

Vitousek PM, Reiners WA (1975) Ecosystem succession and nutrient retention – hypothesis. *Bioscience*, **25**, 376–381.

Wang CK, Bond-Lamberty B, Gower ST (2003) Carbon distribution of a well- and poorly-drained black spruce fire chronosequence. *Global Change Biology*, **9**, 1066–1079.

Waring RH, Landsberg JJ, Williams M (1998) Net primary production of forests: a constant fraction of gross primary production? *Tree Physiology*, **18**, 129–134.

Waring RH, Schlesinger WH (1985) *Forest Ecosystems: Concepts and Management*. Academic Press, Orlando.

Yatskov M, Harmon ME, Krankina ON (2003) A chronosequence of wood decomposition in the boreal forests of Russia. *Canadian Journal of Forest Research-Revue Canadienne De Recherche Forestiere*, **33**, 1211–1226.

Zha T, Barr AG, Black TA *et al*. (2009) Carbon sequestration in boreal jack pine stands following harvesting. *Global Change Biology*, **15**, 1475–1487.

Supporting Information

Additional Supporting Information may be found in the online version of this article:

Appendix S1. Summary file of all data used in Figures 3, 4, 5, 7, 8, 9, and 10.

Please note: Wiley-Blackwell are not responsible for the content or functionality of any supporting materials supplied by the authors. Any queries (other than missing material) should be directed to the corresponding author for the article.